Adsorption of Copper(II) and Mercury(II) Ions onto Chemically-modified Chitosan Membranes: Equilibrium and Kinetic Properties

R.B. Rabelo[1], R.S. Vieira[2], F.M.T. Luna[2], E. Guibal[3] and M.M. Beppu[1]* *(1) School of Chemical Engineering, State University of Campinas, UNICAMP, P.O. Box 6066, 13081-970 Campinas SP, Brazil. (2) Chemical Engineering Department, Universidade Federal do Ceará, UFC, 60455-760 Fortaleza CE, Brazil. (3) Laboratoire Génie de l'Environnement Industriel, Ecole des Mines d'Alès, 6 Avenue des Clavières, 30319, Alès Cedex, France.*

(Received 18 May 2011; accepted 30 October 2011)

ABSTRACT: Cross-linked chitosan was synthesized with glutaraldehyde (chitosan–GLA) and epichlorohydrin (chitosan–ECH). The structures of these matrices were characterized by elemental analysis, Fourier-transform infrared spectrometry (FT-IR), the degree of de-acetylation and the surface topography as determined via scanning electron microscopy (SEM). After promoting interaction with the metal ion, the adsorbent was also studied using FT-IR and energy dispersive X-ray spectroscopy (EDXS). Adsorption studies for Cu(II) and Hg(II) ions were carried out in a batch process. The adsorption kinetics were tested using three models, viz. pseudo-first-order, pseudo-second-order and intra-particle diffusion. The experimental kinetic data were best fitted by the pseudo-second-order model for Cu(II) ions ($R^2 \geq 0.98$) and for Hg(II) ions ($R^2 = 0.99$). Higher rate constants (k_2) were obtained for the adsorption of Cu(II) ions onto chitosan–GLA [1.40 g/(mmol h)] and for Hg(II) ions onto raw chitosan [5.65 g/(mmol h)]. The adsorption rate depended on the concentration of Cu(II) and Hg(II) ions on the adsorbent surface and on the quantity of ions adsorbed at equilibrium. At 293 K, the Langmuir–Freundlich model provided a better fit to the adsorption isotherms on both raw and cross-linked chitosan membranes. The maximum adsorption capacity for Cu(II) ions was obtained with the chitosan–GLA matrix (2.7 mmol/g). A maximum adsorption capacity of 3.1 mmol/g was attained for Hg(II) ions onto the chitosan–ECH matrix.

1. INTRODUCTION

The contamination of aquatic media, particularly by heavy metal ions, is a serious environmental problem which arises mainly as a result of the discharge of industrial waste (Reddad *et al.* 2002). Heavy metal ions are highly toxic at low concentrations and can accumulate in living organisms, causing several disorders and diseases (Gotoh *et al.* 2004). The removal of heavy metal ions from industrial effluents has become a great challenge due to the increasing requirements of environmental regulations.

Copper(II) and mercury(II) ions are well-known toxic heavy metal ions that present a serious threat to fauna and flora fed by water polluted by industrial and urban wastewater, agricultural

*Author to whom all correspondence should be addressed. E-mail: beppu@feq.unicamp.br.

materials and mining. Copper is one of the most largely used metals and Cu(II) ions are reported to be present in metal-bearing industrial effluents (Kannamba *et al.* 2010). The US Environmental Protection Agency has set the maximum contaminant level for Cu(II) ions in industrial effluents as 1.3 mg/ℓ (USEPA 2002). Mercury is commonly found in the global environment and often creates long-term contamination problems; the anthropogenic use of mercury should be reduced, because the difference between tolerable natural background levels of mercury and harmful effects in the environment is exceptionally small (Miretzky and Cirelli 2009). For Hg(II) ions, the maximum uptake level recommended by the World Health Organization is 1 μg/ℓ in drinking water (Wase and Forster 1997).

Several methods exist for the removal of toxic metal ions from aqueous solution, such as membrane filtration, ion exchange, electrolytic methods, reverse osmosis, adsorption, complexation and precipitation (Crist *et al.* 1996; Huang and Blankenship 1984; Juang and Shao 2002). However, these methods have some limitations due to their high operational costs and/or their possible inefficiency in the removal of some toxic metal ions, mainly at trace level concentrations (Reddad *et al.* 2002; Rangel-Mendez *et al.* 2009). Among these methods, adsorption is considered to be an effective and economical process for removing pollutants from wastewater (Wan Ngah *et al.* 2002). Low-cost adsorbents of biological origin such as chitosan and modified chitosan have been used as adsorbents to remove heavy metal ions from groundwater and industrial effluents (An *et al.* 2001; Verbych *et al.* 2005; Zhao *et al.* 2007).

Chitosan, a copolymer primarily composed of poly(1–4)-β-D-glucosamine, is obtained by the enzymatic or alkaline (under heat-treatment) de-acetylation of chitin, a homopolymer of (1–4)-linked *N*-acetyl-β-D-glucosamine residues. Chitosan is a hydrophilic, non-toxic, biodegradable and biocompatible material that has a strong affinity for metal ions (Guibal 2004). This ability arises from the presence of amine and hydroxyl groups on the chitosan chain. Chitosan can bind metal cations by complexation in near-neutral solutions and metal anions by electrostatic attraction/ion-exchange in acid solutions (the protonated amine groups being capable of attracting metal anions).

Several chemical modifications of chitosan have been studied with the aim of improving the metal ion adsorption properties and changing the solubility of chitosan in water or acidic media (Zhao *et al.* 2007). Cross-linking with glutaraldehyde (GLA) or epichlorohydrin (ECH) provides an example of such chemical modifications of chitosan (Monteiro Jr. and Airoldi 1999; Gupta and Jabrail 2006; Koyama *et al.* 1986; Vieira and Beppu 2005). Account should be taken of the fact that cross-linking can reduce the adsorption capacity, especially in the case of chemical reactions involving amine groups, although this loss may be necessary to ensure polymer stability (Miretzky and Cirelli 2009; Bailey *et al.* 1999; Dzul Erosa *et al.* 2001). Depending on the functional groups introduced by the cross-linking agent, the adsorption capacity may increase since the cross-linking process can enlarge the space between chitosan chains, thereby improving the accessibility of amino groups to metal ions (Hsien and Rorrer 1995).

In the present study, chitosan was cross-linked with the purpose of improving its adsorption properties, including its maximum adsorption capacity and kinetic properties. Such modification of chitosan was characterized using FT-IR/ATR methods, elemental analysis and SEM. The kinetics and equilibrium adsorption properties of Cu(II) and Hg(II) ions onto raw and cross-linked chitosan membranes were also investigated. The equilibrium adsorption data were fitted by the Langmuir, Freundlich, Langmuir–Freundlich and Toth models. Kinetic data were modelled by three different models in order to determine the kinetic adsorption rate.

2. EXPERIMENTAL

2.1. Materials

Chitosan (from Sigma), with a de-acetylation minimum of 85% (as extracted from crab shells), was employed. An aqueous solution of glutaraldehyde (25 v/v%) was provided by Nuclear (Brazil). Epichlorohydrin was provided by Merck. Stock solutions of Cu(II) or Hg(II) ions were prepared by dissolving either hydrated copper sulphate ($CuSO_4 \bullet 5H_2O$) or mercuric chloride ($HgCl_2$), which were purchased from Synth and Quimex (Brazil), respectively. All solutions were prepared with de-ionized water (18 MΩ) obtained from a Milli-Q (Millipore) purification system.

2.2. Preparation and chemical modification of chitosan membranes

Porous chitosan membranes were obtained using a method adapted from Zeng and Ruckenstein (1996). Thus, a 2.5 w/w% chitosan solution was spread onto a Petri dish which was maintained at 333 K until a reduction of 50% in its initial weight had been attained. The membranes were then neutralized by immersion in a NaOH solution (1 mol/ℓ) for 24 h, followed by rinsing (using Milli-Q water) and then storing in Milli-Q water at 277 K (Beppu and Santana 2003). Dense films of chitosan were also produced in a similar manner, although total evaporation of the solvent was performed before neutralization. These films were prepared simply for characterization purposes by FT-IR/ATR methods (as required by the analytical procedure).

Raw (pristine) chitosan membranes were cross-linked heterogeneously by immersion in a 0.75 w/w% aqueous glutaraldehyde (GLA) solution (3.0 g of wet chitosan membrane in 50 mℓ of GLA solution) without agitation at room temperature for 2 h, followed by rinsing with de-ionized water to remove any unreacted GLA residue (Hsien and Rorrer 1995). For cross-linking with epichlorohydrin (ECH), the process consisted of immersing 3.0 g of wet raw chitosan membranes in a 0.01 mol/ℓ ECH solution (prepared in 0.067 mol/ℓ NaOH solution) at 313 K under continuous agitation for 2 h (Wei *et al.* 1992). Finally, the membranes were rinsed with de-ionized water to remove unreacted ECH. In this study, chitosan/GLA and chitosan/ECH molar ratios of 5.0 and 0.2 were used, respectively, in accordance with studies by Hsien and Rorrer (1995) and Wei *et al.* (1992).

Some parameters, such as the thickness, diameter and porosity, for raw and cross-linked chitosan membranes have been determined previously by Vieira and Beppu (2006). The water content in the wet chitosan membranes was also determined: 93.9%, 91.5% and 93.1% for raw and GLA- and ECH-cross-linked chitosan, respectively. This conversion factor was very important in calculating the equilibrium and kinetic adsorption results (on the basis of dry weight).

2.3. Elemental analysis

Elemental analysis for both raw and cross-linked chitosan membranes was performed using an elemental analyzer, the main elements of the material — C, H and N — being determined. This experiment was conducted using a LECO CHNS-932 Element Analyzer employing a LECO VTF 900 oxygen pyrolysis furnace. Helium was used as the carrier gas (40 psi), oxygen as the combustion gas (40 psi) and air as the pneumatic gas.

2.4. Equilibrium and kinetic adsorption experiments

Copper(II) or Hg(II) ion stock solutions were prepared by dissolving hydrated copper sulphate ($CuSO_4 \bullet 5H_2O$) or mercuric chloride ($HgCl_2$) in Milli-Q water. These solutions were diluted to obtain standard solutions and were adjusted to the desired pH using NaOH or H_2SO_4 solutions (0.1 mol/ℓ), respectively.

Batch kinetic experiments were undertaken by mixing 7.0 g of wet raw or cross-linked chitosan membranes in 1 ℓ of Cu(II) or Hg(II) ion solution at pH 5.0 and 298 K, and under stirring at 150 rpm. The samples were withdrawn at fixed time intervals and analyzed for their Cu(II) ion or Hg(II) ion content using a Jobin-Yvon JY2000 inductively coupled plasma atomic emission spectrometer (ICP-AES). Only small aliquots of solution were withdrawn for measurement, so as to disturb the system as little as possible and so as not to change the final volume of the solution, thereby influencing the real adsorption phenomena. The chitosan adsorption capacity was calculated by taking into account the variation of the Cu(II) ion or Hg(II) ion solution concentrations at fixed time intervals.

Batch adsorption experiments were carried out by soaking 0.30 g (wet base) of raw or cross-linked chitosan membranes with 25 mℓ of Cu(II) ion or Hg(II) ion solutions at pH 5.0 over a period of 60 h at 293 K and under stirring at 150 rpm. The metal ion concentration in the supernatant was analyzed in each case by ICP-AES methods. The initial metal ion concentration was varied from 50 mg/ℓ to 750 mg/ℓ for Hg(II) ions and from 20 mg/ℓ to 200 mg/ℓ for Cu(II) ions.

The equilibrium adsorbed concentration, Q (mmol/g), was calculated according to the equation (mass-balance equation):

$$Q = \frac{(C_0 - C_e)V}{W} \tag{1}$$

where C_0 (mmol/ℓ) is the initial metal ion concentration, C_e (mmol/ℓ) is the equilibrium metal ion concentration, V (ℓ) is the total volume of the solution and W (g) is the adsorbent mass (in this case, weighed on a wet basis).

2.5. Characterization of metal ion–chitosan complex

2.5.1. FT-IR/ATR spectroscopy

IR spectral analysis was used to confirm the presence of the functional groups in raw and cross-linked chitosan and to observe the chemical modifications after Hg(II) and Cu(II) ion adsorption. Infrared spectra were obtained on chitosan films employing 200 scans and 16 cm^{-1} resolution, employing a Nicolet Protegé 460 (650–4000 cm^{-1}) spectrophotometer equipped with a germanium crystal as the reflection element. The use of the attenuated total reflection (ATR) device allowed information regarding the sample surface to be collected. In order to obtain precise information regarding the extent of Hg(II)–chitosan and Cu(II)–chitosan interaction, dense films were used since they provided better contact between the chitosan surface and the ATR element.

2.5.2. Scanning electron microscopy

The samples were dried under supercritical CO_2 conditions, replacing the fluid filling the membrane pores with supercritical fluid without altering the morphology of the material. Liquid

CO_2 was used since its critical temperature and pressure are relatively low (304 K, 73 bar). The process requires the solvent (i.e. water) to be exchanged with another solvent miscible with liquid CO_2 (such as ethanol). This step was performed sequentially by immersing the chitosan membranes in ethanol solutions at different concentrations (10, 30, 50, 70, 90 and 100 vol%) for 15 min in each case. Thus, the material was placed in an autoclave (Polaron Critical Point Drier) and immersed in liquid CO_2 (293 K, 50 bar). This step allowed the exchange of ethanol contained in the membranes by liquid CO_2. A purge was finally performed to eliminate ethanol from the medium. Increasing the temperature to 304 K and the pressure to 73 bar allowed the CO_2 to reach supercritical conditions. The last step consisted of slowly evacuating the supercritical CO_2 to recover the dry material. Subsequently, the samples were fractured and coated by evaporation with a thin layer of platinum using a sputter coater. Samples were observed using a JEOL JXA-840A scanning electron microscope (JEOL, Japan) at 20 kV under a vacuum of 1.33×10^{-6} mbar.

2.5.3. Energy dispersive X-ray analysis

Energy dispersive X-ray spectroscopy was performed on raw and cross-linked chitosan membranes after metal ion adsorption. The samples were prepared as for the SEM analyses and, in this case, the adsorption of Hg(II) and Cu(II) ion species was performed using a mixed solution of 100 mg/ℓ initial concentration for each species. The objective of this analysis was to qualitatively (not quantitatively) map elemental Hg and Cu on the chitosan surface. The vacuum of 1.33×10^{-6} mbar used could have led to the extraction of mercury. However, the level of the Hg signal observed was still capable of providing a qualitative idea as to the homogeneity of this element on the polymeric matrix.

2.5.4. Mercury and copper speciation

Diagrams of the distribution of mercury and copper species as a function of pH for Hg(II) and Cu(II) ions were simulated using HYDRA (Hydrochemical Equilibrium-Constant Database) software (Puigdomenech 2004). These diagrams were constructed for adsorption at equilibrium concentrations that corresponded to the maximum Hg(II) and Cu(II) ion adsorption.

3. RESULTS AND DISCUSSION

3.1. Properties of chitosan membranes

Table 1 list a series of characteristics of the chitosan membranes studied, the porosity of the chitosan membranes having been determined previously through indirect measurement of the amount of water within the pores (Vieira and Beppu 2006). Zeng and Ruckenstein (1996) proposed a method whose main concept consisted of weighing the wet membranes before and after extracting the water filling the pores. Both a reduction in porosity and a variation in the thickness of the membranes after cross-linking were observed. This was associated with an increase in the hydrophobicity of the membranes as a result of the addition of the alkyl group by the cross-linking reactions. The degree of de-acetylation was measured for each membrane using potentiometric titrations. The corresponding curves presented in our previous study showed that the percentage of amino groups for raw chitosan was 81.0% (Vieira and Beppu 2006). The chitosan–GLA sample did not present a significant amount of proton-binding amino groups. On

TABLE 1. Properties of Raw and Cross-linked Chitosan Membranes

Sample	Thickness (mm)	Diameter (mm)	Porosity (%)	Conversion factor on a dry basis (%)	Degree of de-acetylation (%)
Raw chitosan	1.83 ± 0.07	15.2 ± 0.2	74.7 ± 6.7	93.9	81.0
Chitosan–ECH	1.94 ± 0.05	14.6 ± 0.1	50.7 ± 12.9	91.5	68.7
Chitosan–GLA	1.93 ± 0.12	14.8 ± 0.4	43.9 ± 8.7	93.1	–

the other hand, the chitosan–ECH sample exhibited a proton-binding group percentage which was close to the value found in raw chitosan, i.e. 68.7%. However, the potentiometric titration curve exhibited several inflections, indicating that this cross-linking agent introduced other proton-binding structures besides the original amino groups.

3.2. Elemental analysis

Biopolymer samples were analyzed for their C, N, H and O contents via elemental analysis. The results provided by this analysis for chitosan membranes are listed in Table 2. The elemental amounts as well the C/N and C/O ratio were calculated from these data. Significant changes (chemical modifications) were observed, with the most significant being observed for the chitosan–GLA sample.

The data listed in Table 2 indicate that, after chemical modification with glutaraldehyde, chitosan demonstrated an increased percentage of C and decreased percentages of N and O, while H remained constant. These results are in agreement with the immobilization of the glutaraldehyde molecule which contains approximately 60% of C, 32% of O and 8% of H. For chitosan cross-linked with epichlorohydrin, there was no significant variation in the percentage of C and O related to the addition of epoxy groups in the chitosan structure.

The C/N and C/O ratios changed significantly for chitosan–GLA and to a smaller extent for chitosan–ECH, with the molar ratio used in the cross-linking reaction being higher for chitosan–GLA than for chitosan–ECH. This implies an increase in the percentage of C and a decrease in the percentage of N and O, indicating that cross-linking with glutaraldehyde was more drastic than the reaction with epichlorohydrin. It is possible to compare the experimental and theoretical C/N and C/O ratios, assuming that each molecule of glutaraldehyde or epichlorohydrin bonds to two monomeric chitosan units (see data listed in Table 3, which also includes their respective deviations). Schemes 1 and 2 overleaf present the possible structures obtained after cross-linking using glutaraldehyde and epichlorohydrin, respectively. The substantial deviations between experimental values and theoretical calculations show that the assumption of linkages between two monomeric chitosan units with a single molecule of cross-linking agent was not verified.

TABLE 2. Elemental Analysis of Raw and Cross-linked Chitosan Membranes

Sample	% C	% H	% N	% O
Raw chitosan	41.6	6.8	6.4	44.6
Chitosan–ECH	47.4	7.0	4.8	40.0
Chitosan–GLA	41.8	7.1	6.3	43.8

TABLE 3. C/N and C/O Ratios and Respective Deviations for Raw and Cross-linked Chitosan Membranes

Sample	C/N exp.	C/O exp.	C/N theor.	C/O theor.	% Δ_{rel} C/N	% Δ_{rel} C/O
Raw chitosan	6.50	0.93	6.0	2.0	+8.3	−53.5
Chitosan–ECH	9.88	1.19	8.5	2.83	+16.2	−57.9
Chitosan–GLA	6.63	0.95	7.5	2.14	−11.6	−55.6

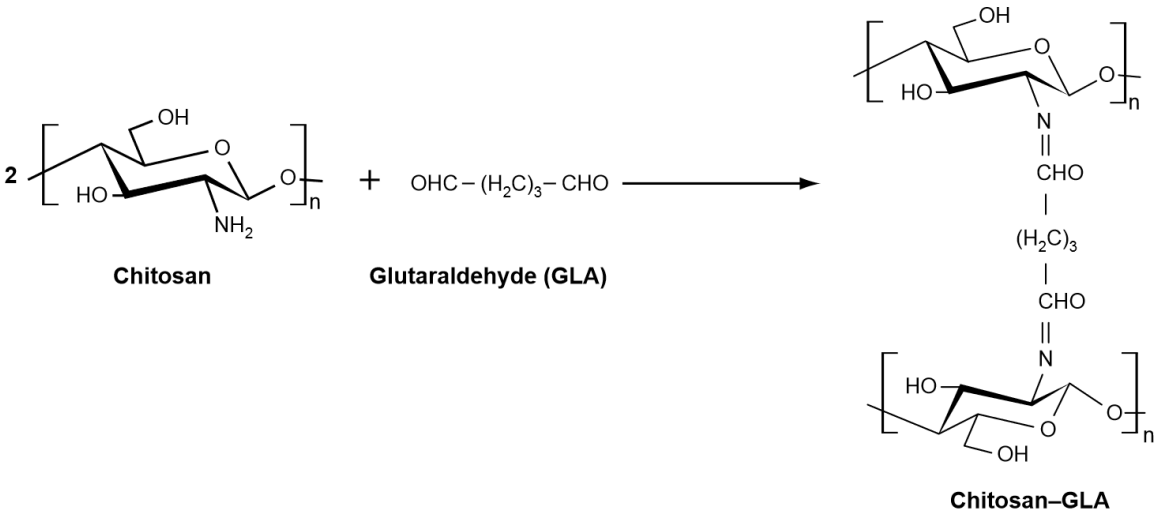

Scheme 1. Possible reaction route for chitosan–GLA cross-linking (Hsien and Rorrer 1995).

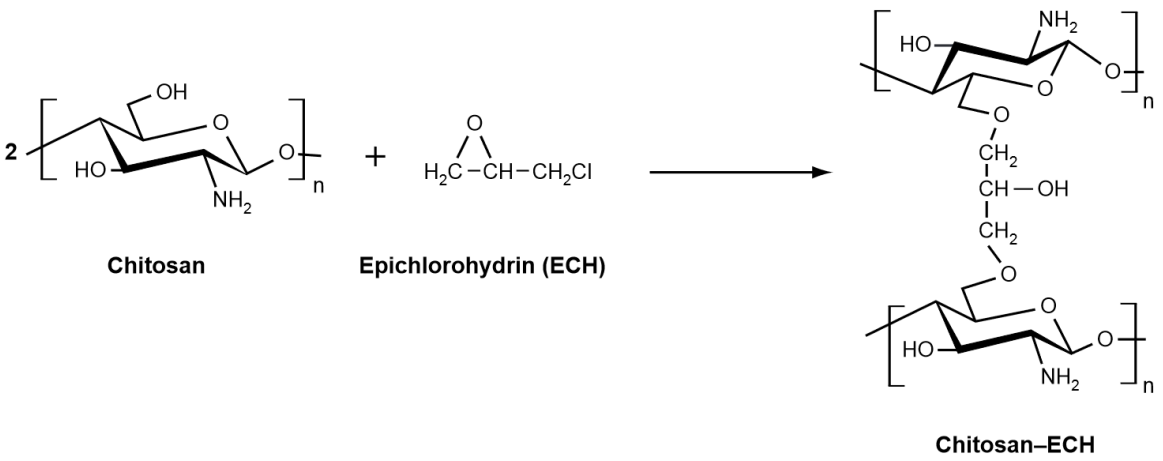

Scheme 2. Possible reaction route for chitosan–ECH cross-linking (Zeng and Ruckenstein 1996).

3.3. SEM analysis

The surface morphology of porous chitosan membranes was analyzed by scanning electron microscopy. All samples were dried under supercritical CO_2 conditions in order to preserve the porous structures of the materials to the greatest possible extent. These results agree with those obtained in a previous study using freeze-drying prior to SEM analysis (Vieira and Beppu 2006). Due to the difficulty in measuring surface area and volume pores in biopolymers, it was not

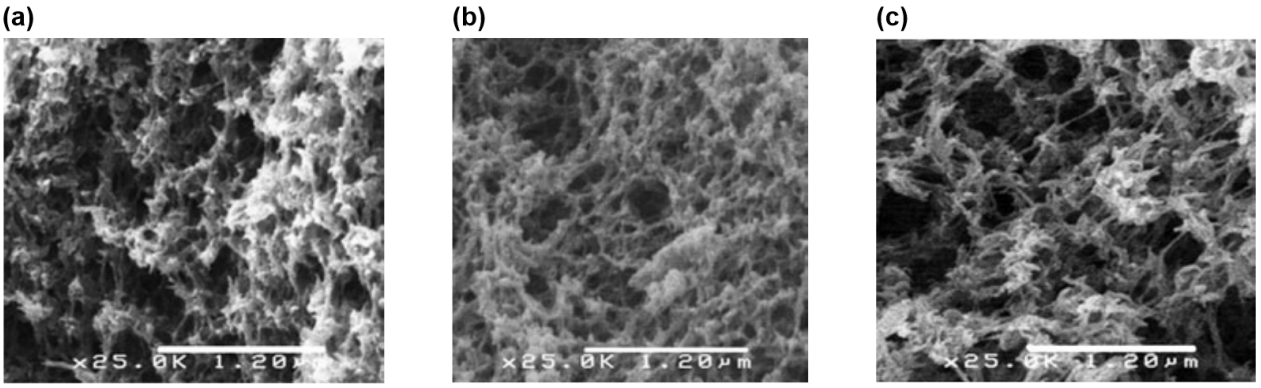

Figure 1. Scanning electron micrographs of the surfaces of (a) raw chitosan, (b) GLA-cross-linked chitosan membranes and (c) ECH-cross-linked chitosan membranes.

possible to make a direct comparison of the most efficient drying method capable of conserving the original porous structure of the material. Figure 1 presents the surface morphology of raw chitosan membranes and of membranes obtained after cross-linking chitosan with glutaraldehyde or epichlorohydrin, respectively.

3.4. EDX spectroscopy

Figures 2–4 show the SEM images and distribution maps of Hg and Cu species on raw chitosan membranes and on membranes obtained after cross-linking chitosan with glutaraldehyde or epichlorohydrin, respectively. A homogeneous distribution of elemental Cu was observed whilst

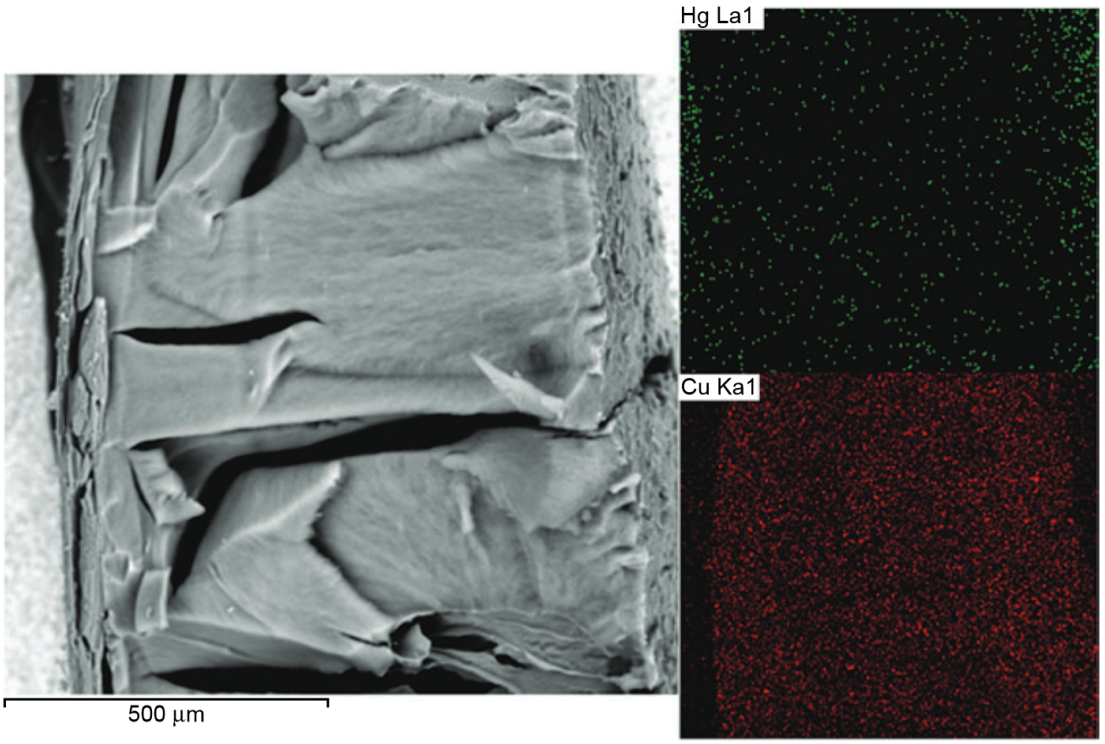

Figure 2. Scanning electron micrographs and energy dispersive X-ray spectroscopy (EDX) maps of elemental Cu and Hg on raw chitosan membranes.

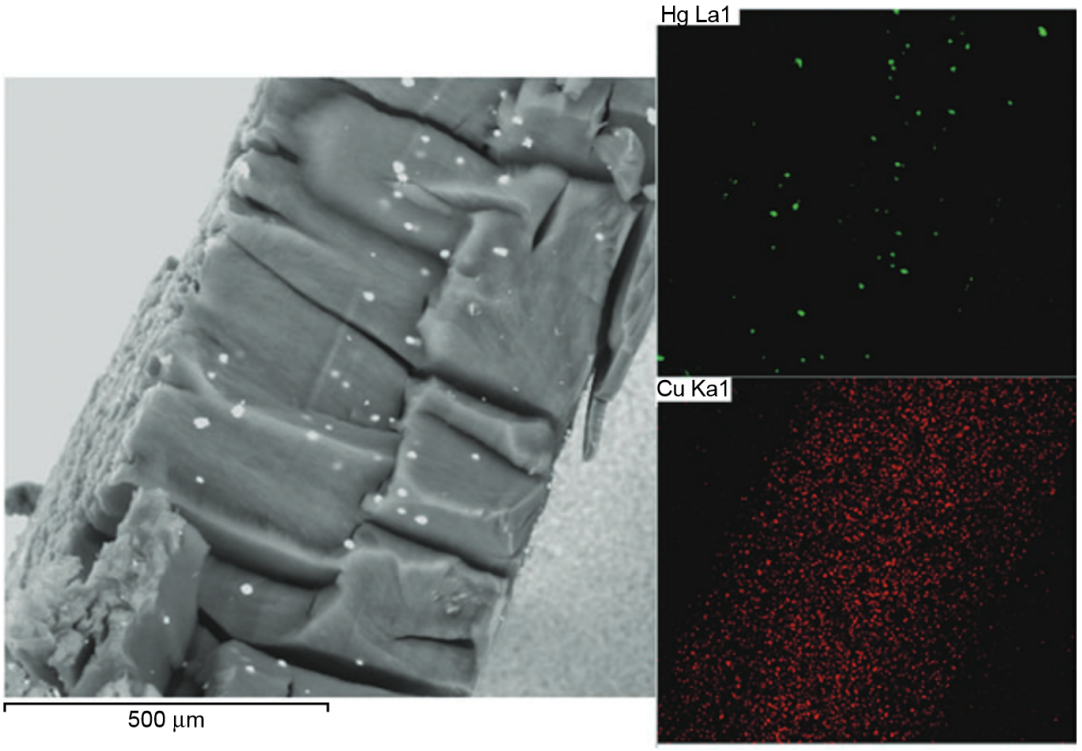

Figure 3. Scanning electron micrographs and energy dispersive X-ray spectroscopy (EDX) maps of elemental Cu and Hg on reticulated chitosan–GLA membranes.

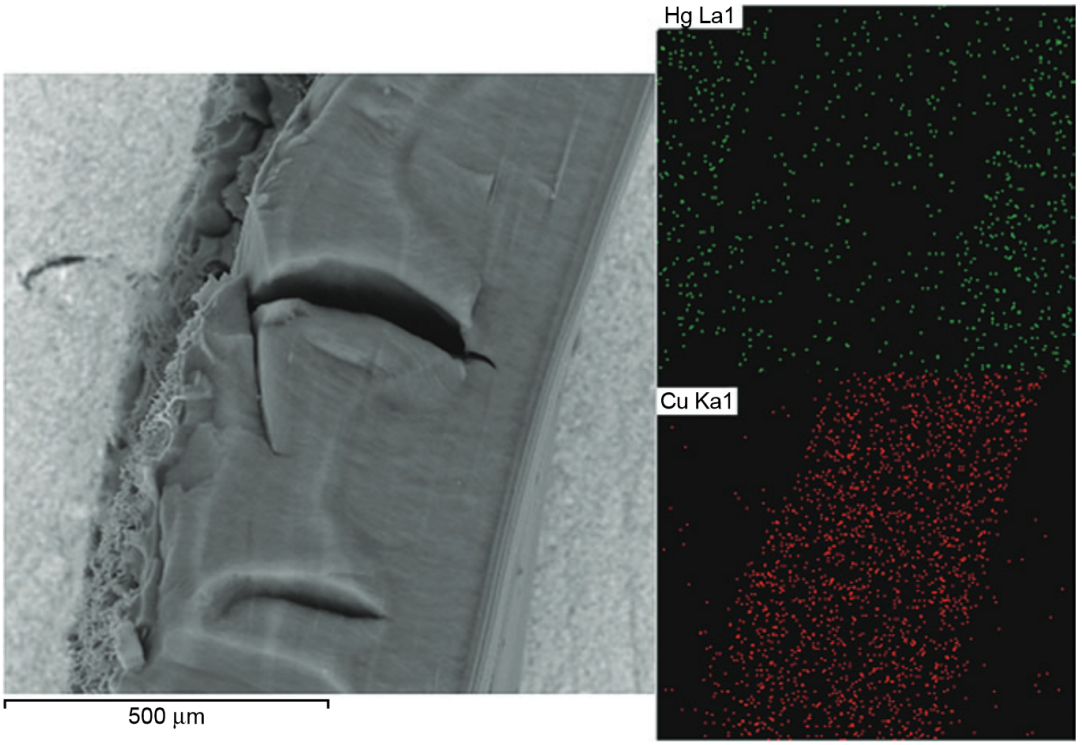

Figure 4. Scanning electron micrographs and energy dispersive X-ray spectroscopy (EDX) maps of elemental Cu and Hg on reticulated chitosan–ECH membranes.

elemental Hg more dispersed, especially for chitosan–GLA. Microphotographs obtained with back-scattered electrons showed that, after adsorption of mercury, the cross-linked membranes with glutaraldehyde exhibited small crystals. This might have arisen from the vaporization or condensation of mercury species in the high-vacuum environment used for the SEM studies. Similar structures to the mercury crystals deposited on chitosan cross-linked with glutaraldehyde have been observed by other workers (Kumaresan *et al.* 1999; Moreno *et al.* 2005; Patil *et al.* 2006).

3.5. FT-IR/ATR spectroscopy

Figures 5(a)–(c) depict the IR spectra for chitosan before and after adsorption. A reduction in the peak associated with the presence of primary amine (1100 cm^{-1}) was observed when chitosan was cross-linked with glutaraldehyde, indicating that these groups were bound to the glutaraldehyde

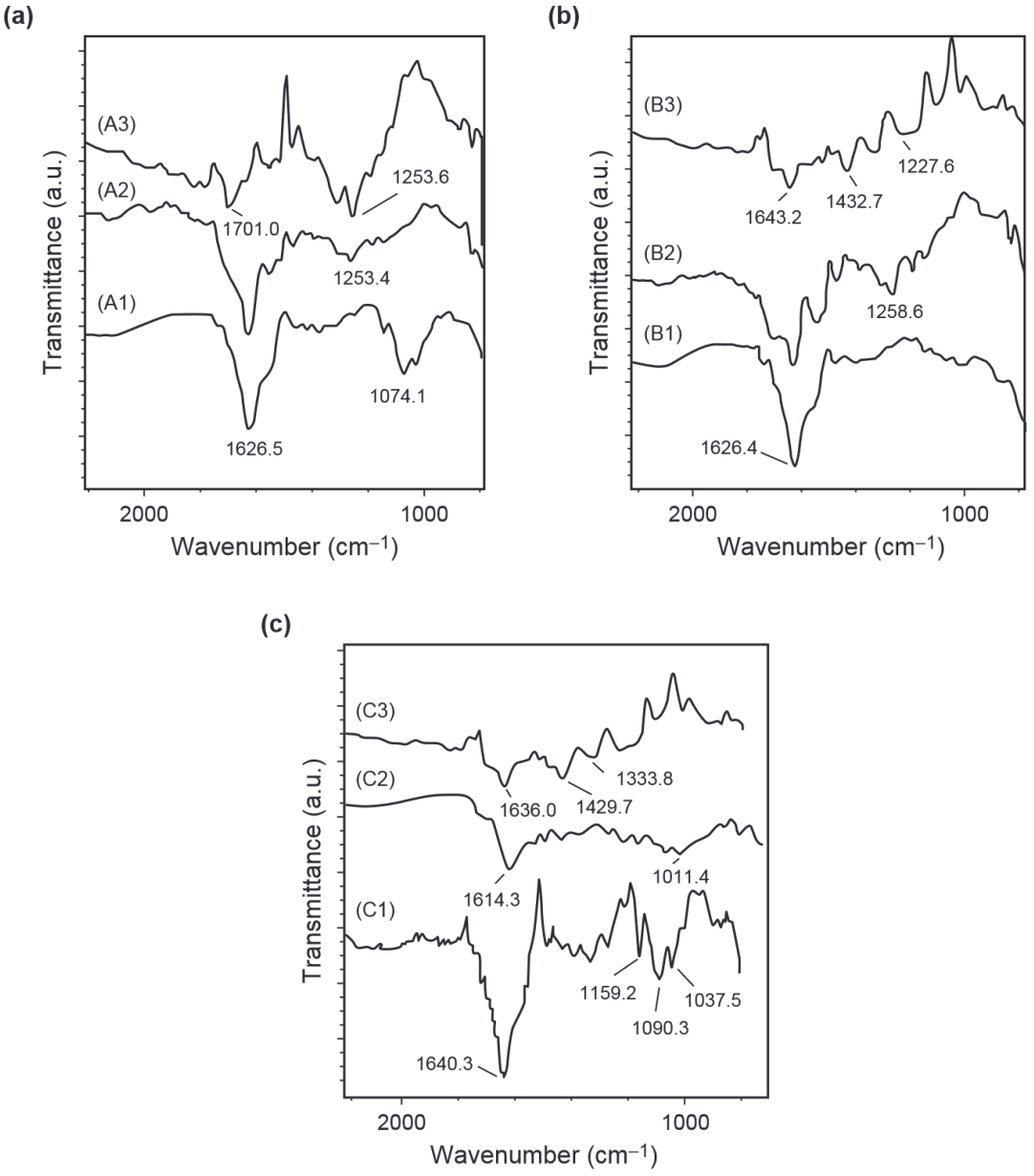

Figure 5. FT-IR/ATR spectra of raw (A1, A2 and A3), glutaraldehyde-cross-linked (B1, B2 and B3) and epichlorohydrin-cross-linked (C1, C2 and C3) chitosan membranes, (a) before, (b) after Hg(II) ion adsorption and (c) after Cu(II) ion adsorption, respectively.

molecules. A peak at 1655 cm^{-1} was also observed. This may be related to the imine bonds (C=N) formed in the cross-linking process (Knaull *et al.* 1999; Koyama *et al.* 1986). There was also evidence of the characteristic band related to the free aldehydic group (1700–1750 cm^{-1}) which did not react with amino groups in the polymer. Particularly, in the case of the extensive cross-linking, both aldehyde groups associated with the bifunctional glutaraldehyde molecules do not necessarily react with chitosan, and hence unreacted aldehyde functions may be available in the final cross-linked matrix.

In the case of chitosan–ECH, an increase in the peak intensity between 1000 and 1300 cm^{-1} was observed, indicating the presence of a C–O bond typical of epichlorohydrin cross-linking. As for the chitosan–GLA sample, a reduction in the peak intensity for the primary amine groups (1100 cm^{-1}) was observed after metal ion binding, indicating that these groups were involved in Hg(II) and Cu(II) ion adsorption. It is, therefore, assumed that the nitrogen atoms are the main adsorption sites for both metal ions. The spectra of chitosan–ECH also presented a reduction in transmittance at 1000–1300 cm^{-1} correlated with the C–O stretching vibrations after metal ion adsorption. These changes suggest that the oxygen atoms of the hydroxyl groups could also be involved in Cu(II) and Hg(II) ion adsorption.

3.6. Mercury and copper speciation

The distribution of mercury and copper species as a function of pH, for a defined metal ion concentration, was simulated using HYDRA (Hydrochemical Equilibrium-Constant Database) software (Puigdomenech 2004) (Figures 6 and 7). A concentration of 50 mg/ℓ corresponds to equilibrium within the range of values used for the determination of both Cu(II) and Hg(II) ion adsorption isotherms. Mercury speciation mainly occurs as $HgCl_2$, $Hg(OH)_2$ and HgClOH at pH 5.0. Under the same conditions, the majority of the Cu(II) ions are present in the free cationic form, such as Cu^{2+}. At a pH value of 5.0, a significant number of the amino groups of chitosan would be protonated as NH_3^+. In this case, the adsorption of Hg(II) ions would be mainly

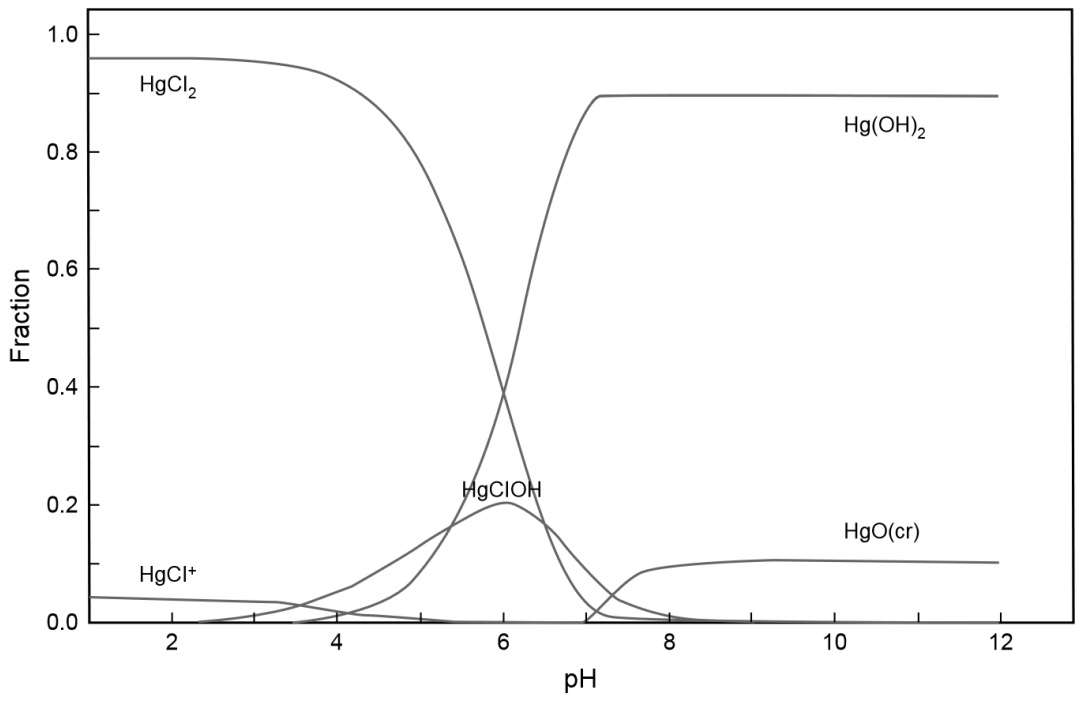

Figure 6. Mercury speciation in aqueous solution as a function of pH (Hg_{total} = 50 mg/ℓ, Cl_{total} = 100 mg/ℓ).

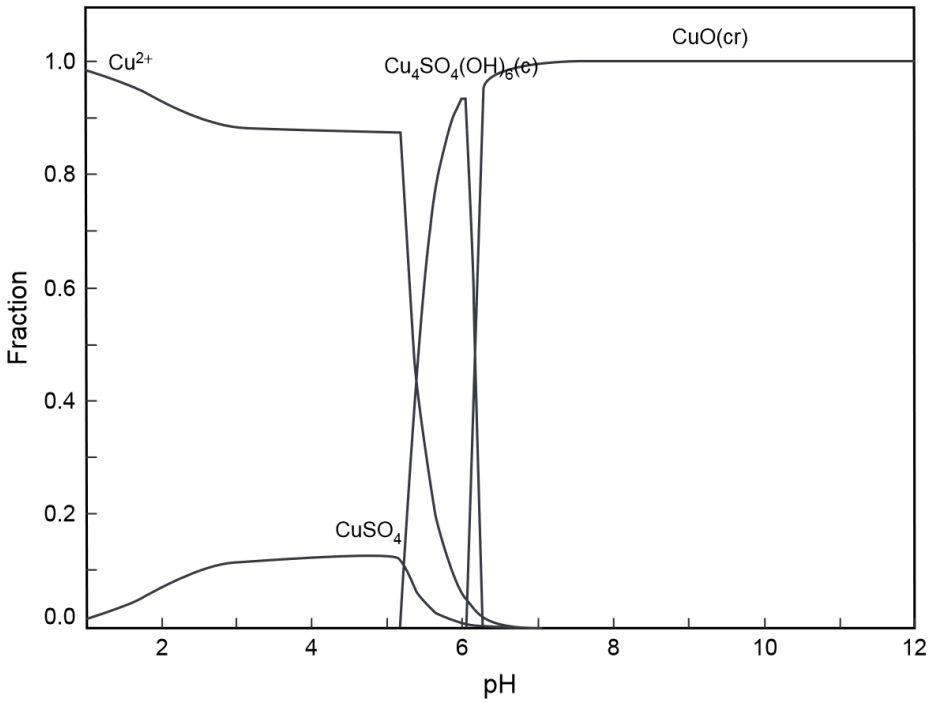

Figure 7. Copper speciation in aqueous solution as a function of pH (Cu_{total} = 50 mg/ℓ, $SO_{4\ total}$ = 50 mg/ℓ).

controlled by electrostatic interaction, in contrast to Cu(II) ion adsorption which would occur by chelation in agreement with the metal speciation.

3.7. Mono-component adsorption results

In order to describe the behaviour of the adsorption isotherm, the Freundlich, Langmuir, Langmuir–Freundlich and Toth models were employed to correlate the equilibrium data. These models may be expressed by the following respective equations (Freundlich 1906; Langmuir 1918; Lazaridis 2003; Toth 1971):

$$Q = K_F C_e^{1/n} \tag{2}$$

$$Q = \frac{Q_{max} K_L C_e}{1 + K_L C_e} \tag{3}$$

$$Q = \frac{Q_{max} \left(K_{L-F} C_e\right)^b}{1 + \left(K_{L-F} C_e\right)^b} \tag{4}$$

$$Q = \frac{Q_{max} K_T C_e}{\left[1 + \left(K_T C_e\right)^{m_T}\right]^{1/m_T}} \tag{5}$$

where K_F [$(mmol^{1-1/n}\ell^{1/n})/g$] is the Freundlich constant that represents the adsorption capacity, 1/n is the heterogeneity factor, Q_{max} (mmol/g) is the maximum adsorption capacity, K_L (ℓ/mmol) is the Langmuir equilibrium constant, K_{L-F} $(\ell/mmol)^{1/b}$ is the Langmuir–Freundlich constant, b is the

Langmuir–Freundlich heterogeneity constant, K_T (ℓ/mmol) is the energy of adsorption of the Toth model and m_T is an empirical constant.

The adsorption isotherm is an extremely important tool for understanding the distribution of the adsorbate on the adsorbent surface at equilibrium (Kannamba *et al.* 2010). Figure 8 depicts the fit of the experimental data obtained in the present study to the different adsorption isotherm models. The simplest adsorption, i.e. the Langmuir model, assumes that (i) the adsorbed molecules form a monolayer on the surface, (ii) there are no interactions between adjacent adsorbed molecules and (iii) each adsorption site is equivalent in terms of adsorption energy (Langmuir 1918).

The Freundlich isotherm is an empirical model used to explain adsorption onto heterogeneous surfaces, which assumes the exponential distribution of active sites and energies. This isotherm does not predict any saturation of the adsorbent surface; thus, infinite surface coverage is predicted, indicating physisorption on the surface (Freundlich 1906; Kyzas and Lazaridis 2009).

One of the most useful extensions to the Langmuir and Freundlich isotherms is the Langmuir–Freundlich equation, which is a general-purpose isotherm for heterogeneous surfaces. The Langmuir–Freundlich model is essentially the Freundlich isotherm with a suitable asymptotic property, in that it approaches a maximum at high concentrations. Moreover, the

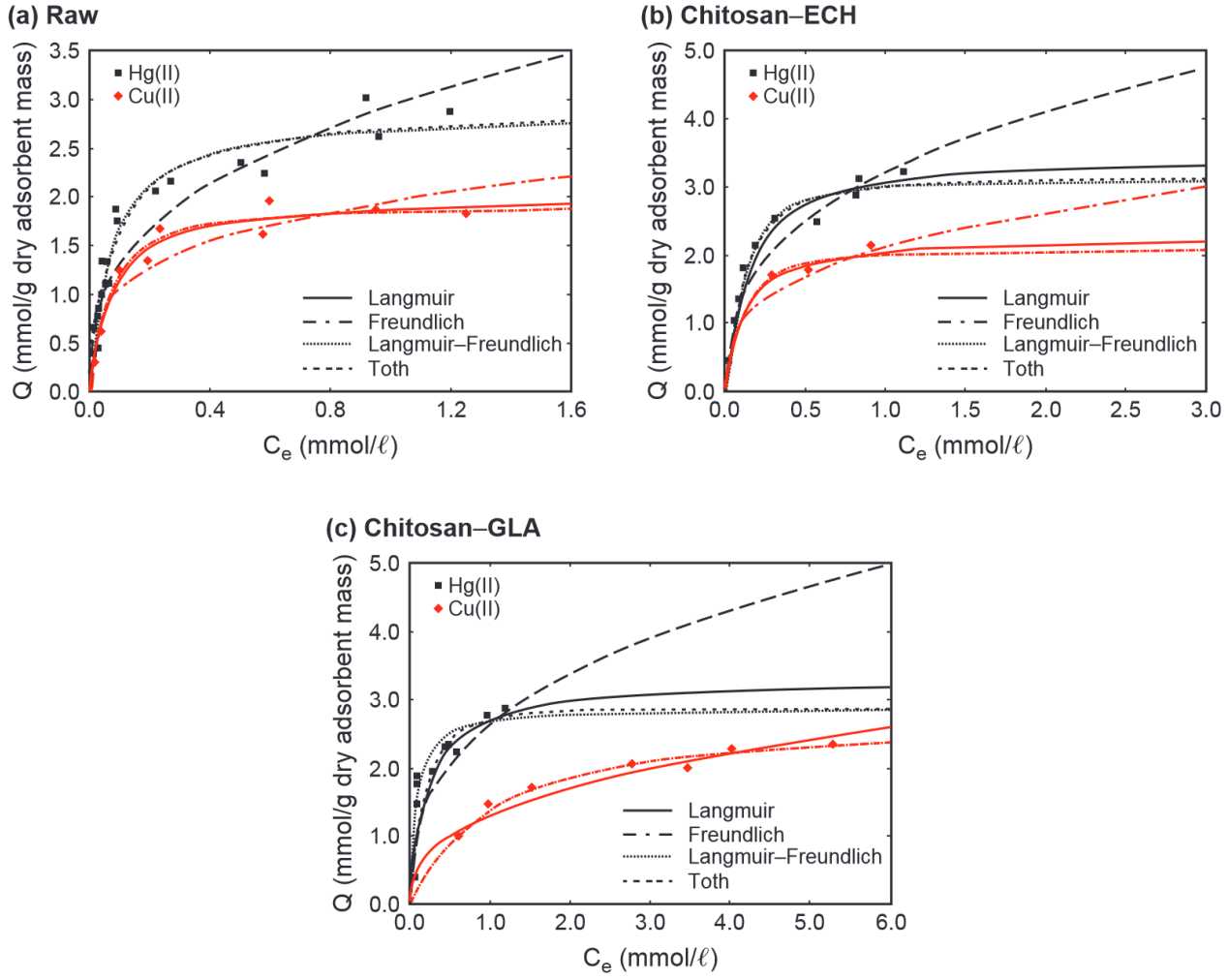

Figure 8. Adsorption isotherms for Hg(II) and Cu(II) ions on (a) raw, (b) glutaraldehyde-cross-linked and (c) epichlorohydrin-cross-linked chitosan membranes at pH 5.0 and 293 K. The symbols correspond to the experimental data while the solid line (—) corresponds to the fit of the Langmuir model, the dashed-dotted line (- · -) to the fit of the Freundlich model, the dotted line (···) to the fit of the Langmuir–Freundlich model and the dashed line (- - -) to the fit of the Toth model.

Langmuir–Freundlich tends towards the Langmuir isotherm when the heterogeneity parameter b is set at unity (Kyzas and Lazaridis 2009).

The Toth isotherm model represents an improvement on the Freundlich and Langmuir adsorption isotherms. This model, derived from potential theory and applicable to heterogeneous adsorption, assumes a quasi-Gaussian energy distribution (Toth 1971; El Mouzdahir *et al.* 2010). Like the Langmuir–Freundlich isotherm, the Toth model tends to the Langmuir isotherm when the energy constant m_T tends to unity (El Mouzdahir *et al.* 2010).

Table 4 summarizes the correlation coefficients, R^2 (used to check the statistical quality of data-fitting), and the various model constants, both obtained via model-fitting employing the

TABLE 4. Parameters of Model-fitting to the Experimental Cu(II) and Hg(II) Ion Adsorption Data.

Langmuir model

	Copper (II)			Mercury(II)		
	Q_{max} (mmol/g)	K_L (ℓ/mmol)	R^2	Q_{max} (mmol/g)	K_L (ℓ/mmol)	R^2
Raw chitosan	2.0 ± 0.1	14.1 ± 2.5	0.955	2.9 ± 0.1	13.7 ± 0.15	0.973
chitosan–GLA	2.8 ± 0.1	1.0 ± 0.1	0.988	3.3 ± 0.1	4.7 ± 0.6	0.977
chitosan–ECH	2.3 ± 0.1	9.1 ± 1.4	0.968	3.5 ± 0.2	7.4 ± 1.3	0.957

Freundlich model

	Copper (II)			Mercury(II)		
	Q_{max} (mmol/g)	K_F [(mmol$^{1-1/n}$ ℓ$^{1/n}$)/g]	R^2	Q_{max} (mmol/g)	K_F [(mmol$^{1-1/n}$ ℓ$^{1/n}$)/g]	R^2
Raw chitosan	2.0 ± 0.1	3.8 ± 0.7	0.838	2.9 ± 0.1	2.9 ± 0.2	0.914
chitosan–GLA	1.31 ± 0.07	2.6 ± 0.3	0.950	2.6 ± 0.1	2.8 ± 0.4	0.886
Chitosan–EC	2.1 ± 0.1	3.2 ± 0.5	0.874	3.2 ± 0.2	2.8 ± 0.4	0.894

Langmuir–Freundlich model

	Copper (II)				Mercury(II)			
	Q_{max} (mmol/g)	$K_{L–F}$ (ℓ/mmol)$^{1/b}$	b	R^2	Q_{max} (mmol/g)	$K_{L–F}$ (ℓ/mmol)$^{1/b}$	b	R^2
Raw chitosan	1.9 ± 0.1	15.6 ± 2.8	1.2 ± 0.2	0.959	2.9 ± 0.1	13.7 ± 2.0	1.0 ± 0.1	0.973
chitosan–GLA	2.7 ± 0.2	1.1 ± 0.2	1.1 ± 0.2	0.988	2.90 ± 0.09	6.2 ± 0.4	1.4 ± 0.1	0.992
chitosan–ECH	2.1 ± 0.1	10.7 ± 1.5	1.3 ± 0.2	0.974	3.1 ± 0.2	9.6 ± 1.5	1.4 ± 0.3	0.965

Toth model

	Copper(II)				Mercury(II)			
	Q_{max} (mmol/g)	K_T (ℓ/mmol)	m_T	R^2	Q_{max} (mmol/g)	K_T (ℓ/mmol)	m_T	R^2
Raw chitosan	1.9 ± 0.1	11.8 ± 3.3	1.3 ± 0.4	0.958	2.9 ± 0.2	14.5 ± 2.6	0.9 ± 0.2	0.973
chitosan–GLA	2.7 ± 0.3	0.9 ± 0.2	1.1 ± 0.3	0.988	2.9 ± 0.1	3.2 ± 0.4	1.7 ± 0.4	0.989
chitosan–ECH	2.1 ± 0.1	7.6 ± 1.6	1.4 ± 0.4	0.972	3.1 ± 0.3	6.3 ± 1.4	1.4 ± 0.6	0.960

least-squares method. The Langmuir–Freundlich model fitted the experimental data well, followed by the Toth, Langmuir and Freundlich isotherm models, respectively. However, the values of the correlation coefficient for the Toth and Langmuir models were very close to that for the Langmuir–Freundlich model. These best fits show that the adsorption sites are not homogeneous (Klepka *et al.* 2008).

According to these results, the Langmuir–Freundlich model gave maximum adsorption capacities of 2.7 mmol/g for the adsorption of Cu(II) ions onto chitosan–GLA and 3.1 mmol/g for the adsorption of Hg(II) ions on chitosan–ECH. Table 5 lists the values of the maximum adsorption capacities of Cu(II) and Hg(II) ions onto different adsorbents as reported in the literature. It may be observed that the values obtained in the present study are close to those achieved with other modified forms of chitosan.

TABLE 5. Adsorption Capacities of Different Adsorbents towards Cu(II) and Hg(II) Ions

Adsorbent	Metal ion	pH	Temp. (K)	Q_{max} (mmol/g)	References
Acid-treated *S. muticum*	Hg(II)	5	298	1.3 ± 0.2	Carro *et al.* (2011)
Sulphated chitosan (S_2C)	Hg(II)	5	293	3.02	Gavilan *et al.* (2009)
Chitosan–ECH	Hg(II)	5	293	3.1 ± 0.2	Present study
Thiourea-modified chitosan	Hg(II)	5	299	6.29	Wang *et al.* (2010)
Banana peel	Cu(II)	4	298	0.9 ± 0.2	Albarelli *et al.* (2011)
Cross-linked chitosan (CHS–H_2fmbme)	Cu(II)	6	298	1.79	Vasconcellos *et al.* (2007)
Chitosan–GLA	Cu(II)	5	293	2.7 ± 0.2	Present study
Cross-linked chitosan (GA-C-ENCS)	Cu(II)	6	293	3.11	Anirudhan and Rijith (2009)

Chitosan membranes showed a higher adsorption capacity towards Hg(II) ions relative to Cu(II) ions. This fact may be correlated with the corresponding ionic radii: Cu(II) (0.73 Å) < Hg(II) (1.02 Å). These results are consistent with those given by Choy and McKay (2005) who used bone char for Cu(II) and Cd(II) ion sorption. They showed that the adsorption capacity for Cu(II) ions was higher than that for Cd(II) ions. This trend follows the reverse order of the radii of the hydrated ions, viz. Cu(II) (4.19 Å) > Cd(II) (4.26 Å) and of the electronegativity, viz. Cu(II) (1.90) > Cd(II) (1.69) (Vieira *et al.* 2007). Nevertheless, it was proportional to the ionic radii [Cu(II) (0.73 Å) < Cd(II) (0.95 Å)] (Vieira *et al.* 2007).

The very high sorption capacities found for cross-linked chitosan may be attributed to the cross-linking treatment, which causes an enlargement in the space between the chitosan chains. This enlargement could ultimately be responsible for improving the accessibility of metal ions to the amino groups (Hsien and Rorrer 1995). For this reason, an increase in the maximum adsorption amount may be interpreted in terms of the decrease in crystallinity caused by cross-linking brought about by the partial destruction of the crystalline structure (Koyama *et al.* 1986; Roberts 1992). Many studies have concluded that when the crystallinity is reduced, the adsorptive capacity is improved (Monteiro Jr. and Airoldi 1999; Kurita *et al.* 1986). Hence, crystallinity plays a fundamental role in the accessibility of adsorbent groups to metallic ions (Kurita *et al.* 1979).

3.8. Adsorption kinetics

Figures 9(a) and (b) overleaf present the adsorption kinetics for Cu(II) and Hg(II) ions onto raw and cross-linked chitosan [initial metal concentration of Cu(II) and Hg(II) ions = 15 mg/ℓ; pH 5.0].

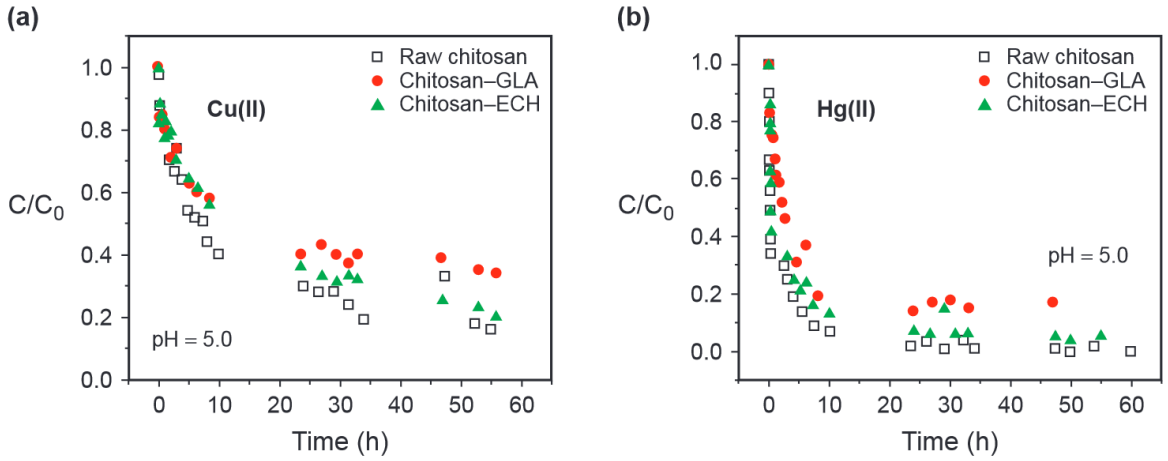

Figure 9. Kinetic data for the adsorption of (a) Cu(II) ions and (b) Hg(II) ions onto raw and cross-linked chitosan membranes. Experimental conditions: initial metal concentration of Cu(II) and Hg(II) ions = 15 mg/ℓ; pH = 5.0.

During the first stage of the process, the rate of adsorption was very rapid and the system tended towards equilibrium, especially for the Hg(II) ions where the equilibrium time was close to 10 h under the experimental conditions employed. However, the second stage of the process was characterized by a slower adsorption rate. For Cu(II) ions, the metal ion concentration in the aqueous phase decreased continuously even after contact for more than 2 d, indicating the existence of a concentration gradient. Thus, the contribution of intra-particle diffusion in the control of uptake kinetics was more significant for Cu(II) ions than for Hg(II) ions. In addition, cross-linking decreased the rate of adsorption of both ions.

The uptake kinetics were modelled using three simplified equations, i.e. pseudo-first-order, pseudo-second-order and intra-particle diffusion. The equation for the pseudo-first-order model may be expressed as (Lagergren 1898):

$$1/Q_t = (k_1/Q_e t) + (1/Q_e) \quad (6)$$

where k_1 is the pseudo-first-order adsorption rate constant (h^{-1}), and Q_e and Q_t (mmol/g) correspond to the amount of metal ions adsorbed at equilibrium and at time t (h), respectively. The value of $1/Q_t$ was calculated from the experimental results and plotted against 1/t.

The pseudo-second-order model is given by equation (7) (Ho and McKay 1999):

$$t/Q_t = (1/k_2 Q_e^2) + (1/Q_e)t \quad (7)$$

where k_2 [(g/(mmol h)] is the pseudo-second-order adsorption rate constant. Similarly, the simplified approach to intra-particle diffusion resistance may be expressed as in equation (8) (Weber Jr. and Morris 1962):

$$Q_t = k_i t^{0.5} \quad (8)$$

where k_i [mmol/(g $h^{1/2}$)] is a parameter representing the gradient of the linear part of the curve. Although this parameter is not usually of the same magnitude as a constant rate, it is characteristic of the rate of adsorption at the start of the process.

Figures 10(a) and (b) and Figures 11(a) and (b) demonstrate the application of the pseudo-second-order kinetic model and the intra-particle diffusion model, respectively, to the experimental data for the adsorption of Cu(II) and Hg(II) ions onto raw and cross-linked chitosan. The values of the adsorption rate constants, k_1, k_2 and k_i were determined from the plots depicted in Figures 10 and 11. Tables 6 and 7 list these values, together with the values of the correlation coefficient, R^2, obtained from the application of the least-squares correlation method. Application of the pseudo-first-order kinetic model did not provide a good fit to the experimental results since the kinetic parameters derived from this model for the adsorption of Cu(II) ions were higher than those for the adsorption of Hg(II) ions. This did not reflect the actual kinetics and the corresponding plots are not depicted in accordance with other studies that showed that it is inappropriate to use this model to correlate the kinetics of the adsorption of metal species over the whole time period of the adsorption process (Lee *et al.* 2001).

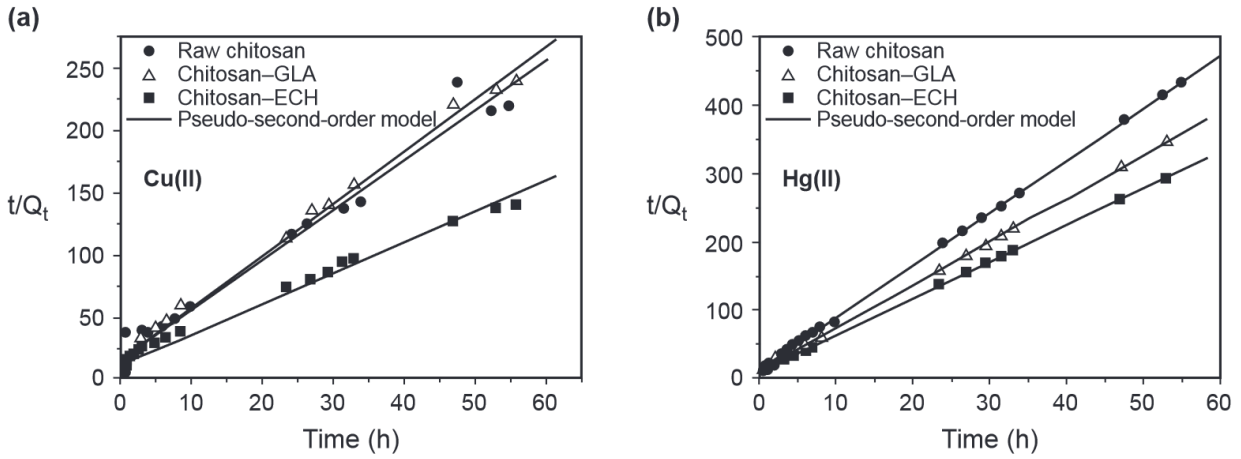

Figure 10. Application of the pseudo-second-order kinetic model to the kinetic data for the uptake of (a) Cu(II) ions and (b) Hg(II) ions onto various chitosan-based membranes. Experimental conditions: initial metal concentration of Cu(II) and Hg(II) ions = 15 mg/ℓ; pH = 5.0.

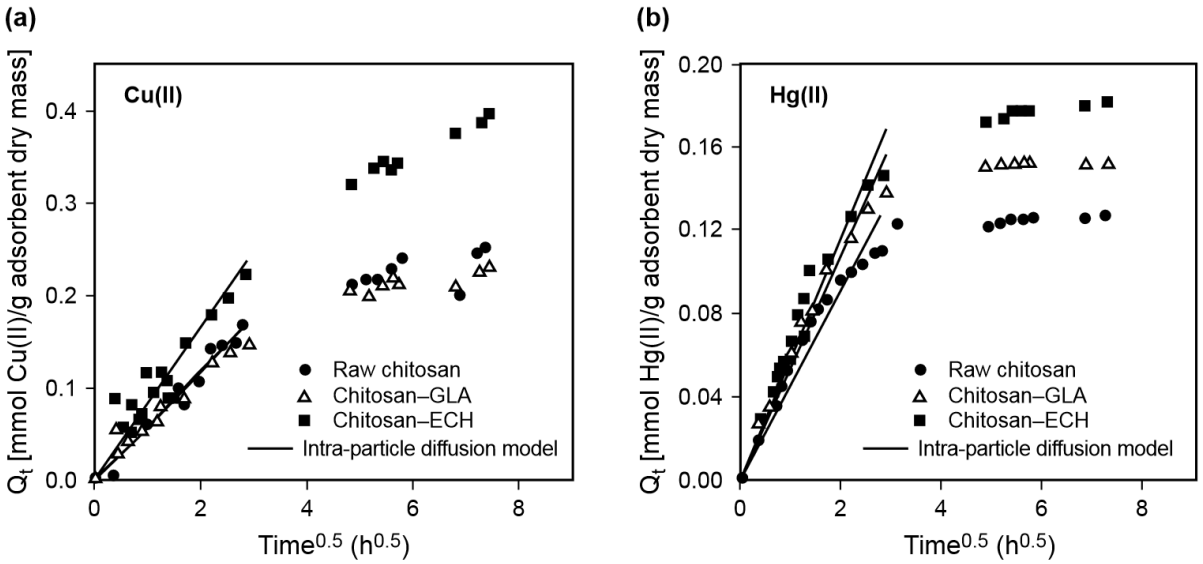

Figure 11. Application of the intra-particle diffusion model to the kinetic data for the uptake of (a) Cu(II) ions and (b) Hg(II) ions onto various chitosan-based membranes. Experimental conditions: initial metal concentration of Cu(II) and Hg(II) ions = 15 mg/ℓ; pH = 5.0.

TABLE 6. Application of Various Kinetic Models to the Data for the Adsorption of Cu(II) Ions and their Corresponding Correlation Coefficients, R^2

	Initial conc.	Pseudo-first-order model			Pseudo-second-order model			Intra-particle diffusion model			
	C_0 (mmol/ℓ)	Q_e (mmol/g)	10^3k_1 (h^{-1})	R^2	Q_e (mmol/g)	k_2 [g/(mmol h)]	R^2	$10^2k_{i.1}$	R_1^2	$10^3k_{i.2}$	R_1^2
Raw chitosan	15	2.86	3.73	0.81	0.13	5.65	0.99	4.47	0.94	1.85	0.56
chitosan–GLA	15	3.26	4.42	0.85	0.16	1.40	0.99	5.35	0.96	–	–
chitosan–ECH	15	3.45	4.31	0.81	0.19	2.98	0.99	5.78	0.93	3.71	0.95

TABLE 7. Application of Various Kinetic Models to the Data for the Adsorption of Hg(II) Ions and their Corresponding Correlation Coefficients, R^2

	Initial conc.	Pseudo-first-order model			Pseudo-second-order model			Intra-particle diffusion model			
	C_0 (mmol/ℓ)	Q_e (mmol/g)	10^3k_1 (h^{-1})	R^2	Q_e (mmol/g)	k_2 [g/(mmol h)]	R^2	$10^2k_{i.1}$	R_0^2	$10^3k_{i.2}$	R_1^2
Raw chitosan	15	1.96	8.77	0.90	0.25	0.91	0.99	5.77	0.97	9.88	0.56
chitosan–GLA	15	2.75	5.16	0.83	0.24	4.59	0.98	5.80	0.85	8.37	0.64
chitosan–ECH	15	2.23	9.60	0.85	0.41	0.55	0.99	8.20	0.88	27.7	0.96

Modelling the experimental data using the intra-particle diffusion model showed the co-existence of two regions, which were characterized by two constants ($k_{i,1}$ and $k_{i,2}$). The values of adsorption rate constant were much higher over the first region, indicating the contribution of two successive and different mechanisms, especially for Hg(II) ions. These different sections may be associated with different physical or chemical constraints, such as the effect of film diffusion resistance, intra-particle diffusion resistance or chemical interaction.

To investigate whether the mechanism was predominantly controlled by diffusion, experiments were undertaken using raw chitosan membranes of different thicknesses (δ_1 = 0.45 ± 0.02 cm, δ_2 = 1.18 ± 0.07 cm, δ_3 = 2.87 ± 0.12 cm). The mass of chitosan and the initial concentration of both ion species (50 mg/ℓ) were kept constant. Figures 12(a) and (b) show the Cu(II) and Hg(II) ion adsorption rates using raw chitosan membranes of different thicknesses. Varying the membrane thickness had a greater effect on the sorption kinetics for Cu(II) ions than for Hg(II) ions, thereby confirming that the effect of intra-particle diffusion was more significant for the Cu(II) ion. The adsorption rate constants arising from the application of the pseudo-second-order model to the experimental data were smaller for Cu(II) ions than for Hg(II) ions, which was directly opposite to the results obtained from the pseudo-first-order model. This indicates that external diffusion (film effect) was less significant than intra-particle diffusion.

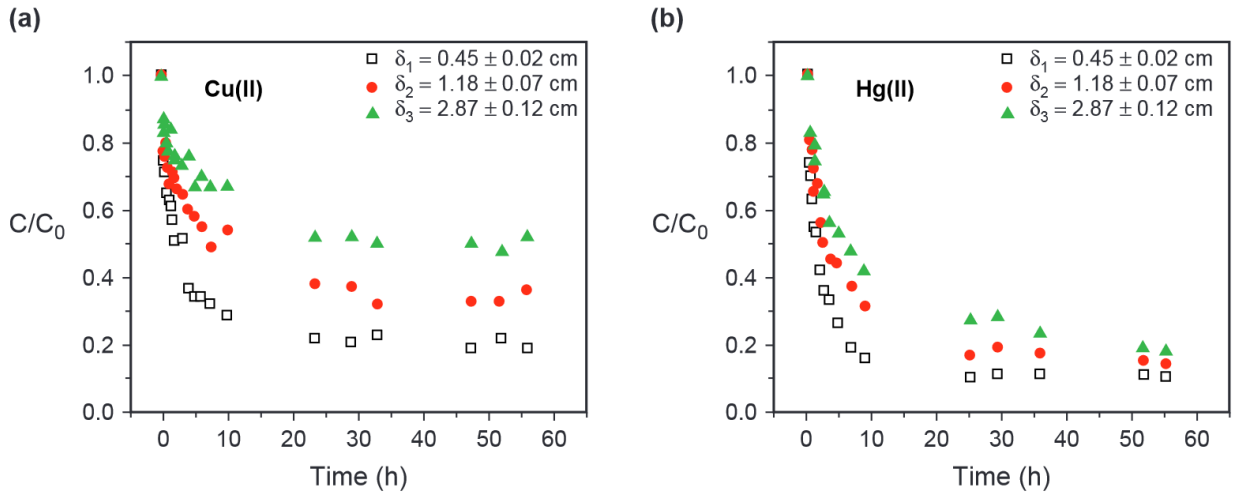

Figure 12. Kinetic plots for the adsorption of (a) Cu(II) ions and (b) Hg(II) ions onto raw chitosan membranes of different thicknesses. Experimental conditions: initial metal concentration of Cu(II) and Hg(II) ions = 15 mg/ℓ; pH = 5.0.

CONCLUSIONS

The adsorption of Cu(II) and Hg(II) ions from aqueous solution onto epichlorohydrin- and glutaraldehyde-cross-linked chitosan membranes was investigated in the present study. Modification of raw chitosan was confirmed by CHN analysis, FT-IR/ATR spectroscopy, EDX and SEM methods. Equilibrium isotherm data were fitted using different models, viz. the Langmuir, Freundlich, Langmuir–Freundlich and Toth models. Of these, the Langmuir–Freundlich model provided the best fit of the experimental data. According to this model, the adsorption capacity of raw and cross-linked chitosan membranes towards Hg(II) ions was greater than that achieved for Cu(II) ions. The maximum adsorption capacity for Cu(II) ions was exhibited by chitosan–GLA (2.7 mmol/g). Similarly, chitosan–ECH exhibited the maximum adsorption capacity for Hg(II) ions (3.1 mmol/g). Kinetic studies showed that the adsorption data

for both metal ions was best fitted by the pseudo-second-order model. These results suggest that the chitosan adsorbents studied could be used in separation processes and that they are capable of adsorbing both Cu(II) and Hg(II) ions from aqueous solution.

ACKNOWLEDGEMENTS

The authors thank FAPESP, Brazil, for financial support and scholarship funding.

REFERENCES

Albarelli, J.Q., Rabelo, R.B., Santos, D.T., Beppu, M.M. and Meireles, M.A.A. (2011) *J. Supercrit. Fluids* **58,** 343.
An, H.K., Park, B.Y. and Kim, D.S. (2001) *Water Res.* **35,** 3551.
Anirudhan, T.S. and Rijith, S. (2009) *Colloids Surf. A* **351,** 52.
Bailey, S., Olin, T., Bricka, M. and Adrian, D. (1999) *Water Res.* **33,** 2469.
Beppu, M.M. and Santana, C.C. (2003) *Mater. Sci. Eng., C* **23,** 651.
Carro, L., Barriada, J.L., Herrero, R. and Sastre de Vicente, M.E. (2011) *J. Hazard. Mater.* **192,** 284.
Choy, K.K.H. and McKay, G. (2005) *Environ. Int.* **31,** 845.
Crist, R.H., Martin, J.R., Chanko, J. and Crist, D.R. (1996) *Environ. Sci. Technol.* **30,** 2456.
Dzul Erosa, M.S, Saucedo Medina, T.I., Navarro Mendoza, R., Avila Rodriguez, M. and Guibal, E. (2001) *Hydrometallurgy* **61,** 157.
El Mouzdahir, Y., Elmchaouri, A., Mahboub, R., Gil, A. and Korili, S.A. (2010) *Desalination* **250,** 335.
Freundlich, H.M.F (1906) *Z. Phys. Chem.* **57,** 384.
Gavilan, K.C., Pestov, A.V., Garcia, H.M., Yatluk, Y., Roussy, J. and Guibal, E. (2009) *J. Hazard. Mater.* **165,** 415.
Gotoh, T., Matsushima, K. and Kikuchi, K.I. (2004) *Chemosphere* **55,** 57.
Guibal, E. (2004) *Sep. Purif. Technol.* **38,** 43.
Gupta, K.C. and Jabrail, F.H. (2006) *Carbohydr. Polym. A* **66,** 43.
Ho, Y.S. and McKay, G. (1999) *Process Biochem.* **34,** 451.
Hsien, T.Y. and Rorrer, G.L. (1995) *Sep. Sci. Technol.* **30,** 2455.
Huang, C.P. and Blankenship, D.W. (1984) *Water Res.* **18,** 37.
Juang, R.S. and Shao, H.J. (2002) *Water Res.* **36,** 2999.
Kannamba, B., Reddy, K.L. and AppaRao, B.V. (2010) *J. Hazard. Mater.* **175**, 939.
Klepka, M.T., Nedelko, N., Greneche, J.M., Lawniczak-Jablonska, K., Demchenko, I.N., Slawska-Waniewska, A., Rodrigues, C.A., Debrassi, A. and Bordini, C. (2008) *Biomacromolecules* **9,** 1586.
Knaull, Z.J., Hudson, S.M. and Creber, A.M.K. (1999) *J. Polym. Sci. B* **37,** 1079.
Koyama, Y., Taniguchi, A., Huang, C.P. and Blakenship, D.W. (1986) *J. Appl. Polym. Sci.* **31,** 1951.
Kumaresan, R., Babu, S.M. and Ramasamy, P. (1999) *Mater. Chem. Phys.* **59,** 107.
Kurita, K., Koyama, Y. and Taniguchi, A. (1986) *J. Appl. Polym. Sci.* **31,** 1169.
Kurita, K., Sannan, T. and Iwakura, Y. (1979) *J. Appl. Polym. Sci.* **23,** 511.
Kyzas, G.Z. and Lazaridis, N.K. (2009) *J. Colloid Interface Sci.* **331,** 32.
Lagergren, S. (1898) *K. Sven. Vetenskapsakad. Handl.* **24,** 1.
Langmuir, I. (1918) *J. Am. Chem. Soc.* **40,** 1361.
Lazaridis, N.K. (2003) *Water Air Soil Pollut.* **146,** 127.
Lee, V.K.C., Porter, J.F. and McKay, G. (2001) *Food Bioprod. Process.* **79,** 21.
Miretzky, P. and Cirelli, A.F. (2009) *J. Hazard. Mater.* **167,** 10.
Monteiro Jr., O.A.C. and Airoldi, C. (1999) *Int. J. Biol. Macromol.* **26,** 119.
Moreno, T., Higueras, P., Jones, T., McDonald, I. and Gibbons, W. (2005) *Atmos. Environ.* **39,** 6409.

Patil, R.S., Lokhande, C.D., Mane, R.S., Pathan, H.M., Joo, O.-S. and Han, S.-H. (2006) *Mater. Sci. Eng., B* **129,** 59.

Puigdomenech, I. (2004) *HYDRA: Hydrochemical Equilibrium-Constant Database Software*, Royal Institute of Technology, Stockholm, Sweden.

Rangel-Mendez, J.R., Monroy-Zepeda, R., Leyva-Ramos, E., Diaz-Flores, P.E. and Shirai, K. (2009) *J. Hazard. Mater*. **162,** 503.

Reddad, Z., Gerente, C., Andres, Y. and Cloirec, P.L. (2002) *Environ. Sci. Technol*. **36,** 2067.

Roberts, G.A.F. (1992) *Chitin Chemistry*, MacMillan Press Ltd., London, U.K.

Toth, J. (1971) *Acta Chim. Acad. Sci. Hung*. **69,** 311.

USEPA (2002) *Lead and Copper Monitoring and Reporting Guidance for Public Water Systems, EPA-816-R-02-009*, Ground Water and Drinking Water Division, Water Programs, US Environmental Protection Agency, Washington, DC, U.S.A.

Verbych, S., Bryk, M., Chornokur, G. and Fuhr, B. (2005) *Sep. Sci. Technol*. **40,** 1749.

Vieira, R.S. and Beppu, M.M. (2005) *Adsorption* **11,** 731.

Vieira, R.S. and Beppu, M.M. (2006) *Colloids Surf. A* **279,** 196.

Vieira, R.S., Guibal, E., Silva, E.A. and Beppu, M.M. (2007) *Adsorption* **13,** 603.

Wan Ngah, W.S., Endud, C.S. and Mayanar, R. (2002) *React. Funct. Polym*. **50,** 181.

Wang, L., Xing, R., Liu, S., Cai, S., Yu, H., Feng, J., Li, R. and Li, P. (2010) *Int. J. Biol. Macromol*. **46,** 524.

Wase, D.A.J. and Forster, C.F. (1997) *Biosorbents for Metal Ions*, Taylor & Francis, London, U.K.

Weber Jr., W.J. and Morris, J.C. (1962) *Advances in Water Pollution Research*, Pergamon Press, New York.

Wei, Y.C., Hudson, S.M., Mayer, J.M. and Kaplan, D.L. (1992) *J. Polym. Sci. A* **30,** 2187.

Zeng, X. and Ruckenstein, E. (1996) *Ind. Eng. Chem., Res*. **35,** 4169.

Zhao, F., Yu, B., Yue, Z., Wang, T., Wen, X., Liu, Z. and Zhao, C. (2007) *J. Hazard. Mater.* **147,** 67.